Biotechnology Reports 35 (2022) e00745

Contents lists available at ScienceDirect

Biotechnology Reports

journal homepage: www.elsevier.com/locate/btre

Research Article

Micropollutant removal capacity and stability of aquaporin incorporated biomimetic thin-film composite membranes

Hilal Yılmaz [a], Melek Özkan [a,*]

[a] Gebze Technical University, Department of Environmental Engineering, Gebze Kocaeli 41400 Turkey

ARTICLE INFO

Keywords:
Aquaporin
Halomonas elongata
Micropollutant
Nanofiltration membranes

ABSTRACT

Aquaporin incorporated nanofiltration membranes have high potential for future applications on separation processes. In this study, performance of biomimetic thin-film composite membranes containing *Halomonas elongata* and *Escherichia coli* aquaporins with different affinity tags for the removal of micropollutants was investigated.% rejection of the membranes for atrazine, terbutryn, triclosan, and diuron varied between 66.7% and 90.3% depending on the type of aquaporin and micropollutant. The highest removal rate was achieved with a membrane containing *H. elongata* aquaporin for atrazine and terbutryn which have methyl branching in their structure. Electrostatic interactions between micropollutants, thin-film layer of the membrane, and tags of aquaporins may also play important role in rejection of micropollutants. Stability experiments showed that biomimetic membranes can be used for six months period without a remarkable decrease in% rejection. Membrane used 24 times for atrazine removal for a year period lost most of its ability to repel atrazine.

1. Introduction

In terms of management of water resources, conventional wastewater treatment was considered to be sufficient to maintain water quality [1]. However, various pollutants with endocrine-disrupting properties (micropollutants or trace organic pollutants) including pesticides and medicinal drugs, are frequently encountered in receiving environments. Micropollutants are chemical substances present in various environments at very low concentrations (from ng/L to μg/L). These groups consist of compounds such as pharmaceuticals, personal care products, steroid hormones, industrial chemicals, pesticides, polyaromatic hydrocarbons, and by-products of disinfection [2]. Micropollutants are difficult to identify and analyze due to their wide variety, trace concentration, and lack of measurement methods. Micropollutant concentrations in aquatic environments that reach critical levels cause aquatic ecosystem deterioration due to several adverse effects, including short and long-term toxicity [3,4]. Besides, there are still many micro-contaminants with unknown negative effects on living organisms. The stable structure of many trace organic pollutants and their continuous entry into the facilities make it difficult to decrease their concentrations to a safe level [5].

There is an intensive effort on the discovery of novel products and the development of new technologies to improve the wastewater treatment processes in terms of micropollutant removal. For a better micropollutant elimination, alternative treatment methods such as coagulation-flocculation, activated carbon, adsorption (powdered activated carbon and granular activated carbon), and advanced oxidation processes (AOP) are used. Interference of micropollutant adsorption on activated carbon by additional chemicals in the process [6] or formation of by-products which can be more toxic than micropollutant itself in advanced oxidation process [7] is reported problems waiting to be solved. Bioremediation with microalgae is regarded to be one of the most effective environmentally friendly processes for micropollutant removal due to the high surface area and binding affinity of these organisms [8]. The fact that each microalgae species can degrade different types of contaminants exert limitations on bioremediation processes. It is recommended that more studies on discovering novel species are necessary for resistant micropollutants [9].

Membrane filtration, which is regarded to be clean technology as compared to the chemical processes, is preferred for wastewater treatment because of less energy requirement, no use of chemicals during operation, ease of scale-up, and continuity [10]. Polymeric membranes are widely used for water purification and are also commercially available. Membrane technologies have also been applied for removing micropollutants from water and wastewater recently.

Nanofiltration membranes are effective at separating various sized

* Corresponding author at: Environmental Engineering Department, Gebze Technical University: Gebze Teknik Universitesi, Turkey.
E-mail address: mozkan@gtu.edu.tr (M. Özkan).

https://doi.org/10.1016/j.btre.2022.e00745
Received 28 March 2022; Received in revised form 2 June 2022; Accepted 4 June 2022
Available online 9 June 2022

contaminants with different functionalities. It is thought that challenges on the permeability-selectivity tradeoff of existing nanofiltration membranes can be overcome by a biomimetic approach [11]. The unique structures possessed by living organisms, which have successfully completed their evolutionary process, inspire the development of novel materials. The cell membrane is a perfect example of such a structure with extraordinary properties necessary to protect the cell. Membranes of living organisms have high selectivity for substrate and water transport and can achieve high transport rates that are unprecedented in synthetic systems [12]. Aquaporins located in almost all cell membranes facilitate water molecules (and/or other small neutral molecules) to transfer efficiently through the cell membrane [13]. It is determined that 10^9 water molecules per second can be transported by each aquaporin channel thus repelling all other solutes [14]. It has been shown that the permeability and selectivity of traditional thin-film composite (TFC) membranes can be substantially enhanced by inserting aquaporins into polymeric membranes [15].

E. coli AQP-Z is widely used for the fabrication of biomimetic membranes, they are embedded in liposomes deposited on the surface of polyethersulfone (PES) membrane during the interfacial polymerization of TMC and MPD [16–18]. Aquaporin embedded commercially available forward osmosis membranes were also fabricated with this method [19]. Few studies have yet explored the potential of aquaporin incorporated membranes in the elimination of micropollutants in wastewater. The present study aims to determine the efficiency of biomimetic membranes containing aquaporins from a halophilic bacterium, *H. elongata* on micropollutant removal from aqueous environments and compare its rejection potential with that of *E. coli* aquaporin Z incorporated membranes. Aquaporin of *H. elongata* was cloned, produced, and used for TFC membrane fabrication in our previous study. The incorporation of this aquaporin into the membrane structure improved the water flux without decreasing salt rejection potential [20].

2. Material and methods

2.1. Synthesis and purification of aquaporin protein

E. coli BL21 transformants carrying the *E. coli* and *H. elongata* aquaporin genes (Table 1) were cultivated in Luria Broth containing 100 μg/mL ampicillin for GST tagged aquaporins and 25 μg/mL kanamycin for His-tagged one. The culture was cultivated overnight and induced for 3 h with 1 mM IPTG. Membrane protein isolation was conducted as previously described [20,21]. Cells were harvested and lysed by sonication 30 times at 4 °C in pulsed mode for 1 min at 50% duty cycle using an ultrasonic processor (Hielsher, Germany). Cell debris was removed by sedimenting at 12,000 x g at 4 °C for 30 min. To pellet the membrane fraction, the supernatant was centrifuged for another 1 h at 100,000 x g. The membrane fraction was solubilized overnight in a buffer containing 5% Triton-X, 100 mM K_2HPO_4 (pH 7.0), 200 mM NaCl, 10% glycerol and 2 mM β-mercaptoethanol (βME). The supernatant was passed through 0.45 μm sterile filter. The purified proteins were separated with suitable elution solutions from affinity columns and analyzed by SDS-PAGE. For purification of GST-labeled aquaporin, the supernatant was passed through a glutathione sepharose 4B (GE Healthcare) column. The resin was scrubbed with up to 30-bed volumes of a buffer including 100 mM K_2HPO_4 (pH 7.0), 1% Triton-X, 200 mM NaCl, 10% glycerol, and 2 mM βME. With a similar buffer, including reduced L-glutathione and glycerol, the protein was eluted. For purification of His-tagged aquaporin, the supernatant was passed through the column using HIS-Select Cobalt Affinity Gel (Sigma-Aldrich). The resin was scrubbed with up to 30-bed volumes of a buffer including 50 mM Na_2HPO_4 (pH 8.0), 1% Triton-X, 0.3 M NaCl, and 10 mM imidazole. Proteins were eluted with elution buffer comprising 50 mM Na_2HPO_4 (pH 8.0), 1% Triton-X, 0.3 M NaCl, and 250 mM imidazole. SDS-PAGE was conducted for protein profile analysis. The amounts of proteins were calculated by Bradford Assay [22].

Table 1
Aquaporin proteins used in this study.

	Abbreviation	Cloned in vector	Reference
GST tagged *E. coli* aquaporin Z	EcAq	pGEX-4T2	[20]
GST tagged *H. elongata* aquaporin	HeAq1	pGEX-4T2	[20]
His-tagged *H. elongata* aquaporin	HeAq2	PET28a	[21]

2.2. Preparation of liposomes and proteoliposomes with aquaporins

Liposomes have been produced using the thin-film rehydration method [18,23]. In the experiments, DOPC bilayers were formed by Avanti Polar Lipids INC. Liposomes have been prepared by dissolving lipids with a certain amount of chloroform. As a consequence of the depletion of chloroform with N_2 gas, lipids formed thin film in the round bottom flask. In order to reach a final concentration of up to 20 mg/mL, the dried lipid film was rehydrated in 1 mL of phosphate-buffered saline (PBS) and 1% OG (Sigma-Aldrich, USA) incubated at 10 °C for one hour. At the end of one hour, BioBeads (Bio-Rad Laboratories, Inc., USA) was applied to remove the detergent and the mixture obtained was incubated for an hour. The final solution was extruded 21 times through a 200 nm pore size polycarbonate membrane. For proteoliposome preparation aquaporins were included during the rehydration step. The protein-lipid ratio was applied as 1:400 (w/w).

2.3. Determination of water permeability of aquaporins

The sizes of liposomes and proteoliposomes were determined using a Nano Zetasizer. SX20 Stopped Flow Light Scattering Spectrometer (Applied Photophysics, UK) was used to test the water permeability of liposomes. Light scattering measurements were produced using the fluorescence kinetic mode and a 590 nm light source. Vesicles were rapidly mixed with an osmotic draw solution (0.85 M NaCl) driven by 4 atm pressurized nitrogen gas. When mixed with the hypertonic NaCl solution, liposomes expel the water they hold owing to the osmolarity difference. The velocity of the water outlet has been measured by light scattering. When aquaporins are incorporated, water released from liposome's is expected to be higher than that of empty liposomes. The velocity of water production is directly proportional to the k value determined from the measurement. The rate constant k was determined by curve fitting of the stopped-flow spectrometer light scattering results with single order exponential. The reported k values are the averages obtained from 5 to 8 independent stopped-flow measurements. The permeability of the DOPC lipid vesicles was calculated by the equation below [24]:

$$P_f = \frac{r_0}{3 \cdot V_w \cdot T} \cdot \frac{c_{in,0} + c_{out}}{2 \cdot c_{out}^2} \quad (1)$$

where r_0 is the vesicle radius, V_w is the partial molar volume of water (18 cm^3/mole), τ is the time constant $C_{in,0}$ is the initial osmolyte concentration inside the vesicle, and C_{out} osmolyte concentration in the external solution [24].

2.4. Preparation of thin-film composite nanofiltration membranes

Insertion of proteoliposomes on the polysulfone membrane (PS) (Microdyn Nadir Rm UP010) was carried out according to [18]. The solution used to coat the polysulfone membrane contains 1% MPD 0.1% SDS, and proteoliposome solution. The concentration of the TMC solution used is 0.1% in n-hexane.

The membranes were held in the tap water washing through the night at the end of this system to eliminate excess monomers. The membranes were preserved in water from Milli-Q. Coated membranes containing proteoliposomes are illustrated in Fig. 1.

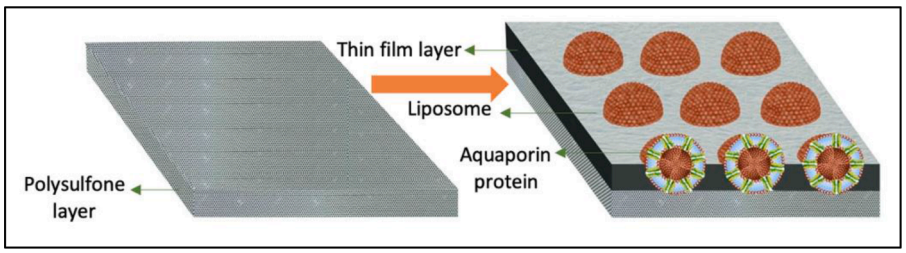

Fig. 1. Membrane structure. TMC-MPD thin film layer was formed on the surface of the polysulfone membrane. Proteoliposomes carrying aquaporins were embedded in the thin film layer. In the control membrane, liposomes without aquaporins were incorporated.

2.5. Characterization of membranes

An attenuated absolute reflection Fourier-transform infrared spectrometer (ATR-FTIR) has been used to analyze the characteristic functional peaks on the thin film layer of the membranes. The infrared spectra were recorded at room temperature in the wavenumber range of 3500 to 500 cm^{-1} using Perkin Elmer Spectrum. The surface layer of the membranes was analyzed by using a Scanning electron microscope (Philips XL30 SFEG, Amsterdam). The water contact angle has been determined using an automated contact angle meter. Membrane surface and incorporated proteoliposomes were analyzed by using SEM (Philips XL30 SFEG, Amsterdam). Membrane pore size analysis was performed using the Quantachrome Porometer 3 G ZH instrument. On both sides, membranes were cut and tightened. The total area was determined and entered into the software as input. The pore size data were acquired using a computer once the measurement was completed [25].

2.6. Measurement of micropollutant removal capacity of membranes

In reverse osmosis (RO) mode, the Sterlitech Company dead-end membrane device (HP4750, USA) was used in the filtration experiments. The membrane area was14.6 cm^2 and 250 mL of feed solution was used. The membrane was placed onto a dead-end porous disk, then the equipment was assembled. 5 bar pressure was applied to filter the feed solution and sample was stirred at 300 rpm during filtration. The amount of filtrate was measured by a precision scale. With the equation given below (Eq. (2)), the flux was determined.

$$Jv = \frac{Qp}{A(system)} \tag{2}$$

Qp is permeated flow (L/h), and A (system) is the membrane system's surface area (m^2). The following equations are used to measure the A (water permeability) (Eq. (3)), R (rejection) and B (salt permeability) values Eq. (4) :

$$A = \frac{Jv}{\Delta P - \Delta \pi} \tag{3}$$

$$B\left(\frac{1}{R} - 1\right) \times Jv \tag{4}$$

Jv is flux, P is the strain exerted and P is the difference in osmotic pressure around the membrane.

$$R = \frac{(Cf - Cp)}{Cf} \times 100 \tag{5}$$

R is the Rejection value (rejection percentage) , Cp, and Cf are salt concentrations in permeate and feed solutions, respectively.

2.7. Determination of micropollutant concentrations using HPLC

Diuron, terbutryn, and triclosan were tested in HPLC (Lab Alliance) using a 288 nm UV detector. The mobile phase used for this experiment was made up of 70% acetonitrile, and 1% TFA (trifluoroacetic acid). In experiments with atrazine, a UV detector at 254 nm was used. 65% acetonitrile 35% 20 mM phosphoric acid solution was used in the mobile process.

2.8. Statistical analysis

All filtration experiments were performed 2 times and the means and standard deviations of flux and rejection parameters (mean ± SD) were calculated at a 95% confidence interval. These results were compared using an independent unpaired *t*-test using MS Excel. Statistical significance of the difference between membrane permeability and rejection capability is evaluated by the value of p. It was observed that the p-value was less than 0.05. The $p < 0.05$ value indicates a statistically significant difference.

2.9. Docking analysis

3D structural modeling is performed by comparison of target amino acid sequence of aquaporin similar protein sequences that have protein database code (PDB code). Phyre2 Server (https://www.sbg.bio.ic.ac.uk/~phyre2) was used for 3D modeling. 1RC2 PDB encoded protein was used as a template for *H. elongata* aquaporin. Protein with a PDB code of 2ABM was used for *E. coli* aquaporin. MOLEOnline program was used to determine the aquaporin channel properties [26]. Docking of aquaporin with different micropollutants including atrazine, diuron, terbutryne, and triclosan was modelled using the Schrödinger's Maestro package (Schrödinger Release 2021–4: Maestro, Schrödinger, LLC, New York, NY, 2021).

3. Results

Thin-film composite membranes in this study were prepared using two different recombinant aquaporins, from *E. coli* and *H. elongata*. Aquaporins include affinity tags for facilitating purification. In this study GST (glutathione S transferase) tagged and His-tagged *H. elongata* aquaporins (HeAq1 and HeAq2, respectively) and GST tagged *E. coli* aquaporin (EcAq) were purified and used for membrane preparation (Table 1). The study not only compares the efficiencies of biomimetic membranes prepared with *E. coli* and *H. elongata* aquaporins for micropollutant rejection but also gives an idea about the effect of different cloning and expression strategies on the activity of aquaporins in membrane structure. Effect aquaporin 3D structures, structure of membrane in terms of pore size and hydrophobicity, and chemical nature of micropollutants were also considered for analysis of rejection performances of the membranes.

3.1. Characterization of proteoliposomes

Before incorporating into the membrane structure, proteoliposomes carrying the aquaporins were characterized and water transfer rates of purified aquaporins were measured. Aquaporin: liposome ratio was applied as 1:400 (P/L(w/w) = 1/400) in proteoliposomes. Normalized

light scattering graphs were obtained from stopped-flow spectrometry measurements. Fig. 2 shows osmotic gradient-driven changes in light scattering for EcAq, HeAq1, HeAq2 containing liposomes and control (empty) liposomes. The intensity of scattering is affected by the size and refractive index of the vesicle. The mechanism of this light scattering was explained in the literature as the concentration of entrapped osmolytes increases after a hyperosmotic shock due to a reduction in vesicle volume. This rise in interior osmolarity raises the refractive index of the vesicle, which improves its light scattering capabilities. At the same time, vesicle size decrease, which reduces scattering capacity, and mitigates this impact [24]. The size of prepared DOPC liposomes and proteoliposomes are shown in Table 2. The vesicles exhibit a size range from 117- 163 nm, accompanied by low polydispersion. Liposomes without aquaporins display a much lower light scattering rate (k) and water permeability (P_f) than proteoliposomes containing aquaporins. *H. elongata* aquaporin incorporated proteoliposomes has higher permeability than *E. coli* aquaporin incorporated ones. This result is consistent with our previous findings [20]. P_f values of aquaporins calculated according to Eq (1) were compared with those of different microbial species including *Rhodobacter sphaeroides*, (RsAqpz), *Escherichia coli* (AqpZ), *Trichoderma atroviride* (TriatXIP), and also a human aquaporin (AQP2) were compared in Table 3. The highest P_f value belongs to *R. sphaeroides* (123×10^{-14} cm^3 /s) (Table 3).

Table 2
Characterization of DOPC liposomes and proteoliposomes.

	Mean diameter of vesicles (nm)	Poly-dispersion index (PDI)	k (s^{-1})	P_f (cm/s) $*10^{-3}$
Liposomes (Control)	163	0.084	23.00	2.48
Proteaoliposomes (EcAq)	152	0.090	56.21	4.23
Proteaoliposomes (HeAq1)	132.3	0.093	69.00	4.53
Proteaoliposomes (HeAq2)	117.5	0.078	60.52	3.53

Table 3
Comparison of water permeability of different aquaporins.

Aquaporins	P_f (cm^3/s)*10^{-14}	References
AqpZ from *E. coli* (GST tagged)[1]	7.9	This Study
Aqp from *H. elongata* (GST tagged)[2]	6.01	This Study
Aqp from *H. elongata* (His-tagged)[3]	2.84	This Study
RsAqpZ from *Rhodobacter sphaeroides*	123	[27]
AQP2 from human	9.89	[28]
AqpZ from *E. coli*	13	[29]
TriatXIP from *Trichoderma atroviride*	2.7	[30]

1,2, and 3 are abbreviated as EcAq, HeAq1, and HeAq2 respectively.

3.2. Characterization of biomimetic membranes

Proteoliposomes and liposomes (for the control membrane) were incorporated on the surface of the membranes as described in the materials and methods section. Bonding pattern change after aquaporin incorporation was detected by using FTIR, the hydrophilicity of the membranes was determined by contact angle measurement, and the surface and cross-section of the membranes were visualized by SEM analysis. Typically, the water contact angle defines the hydrophilicity of the membrane surface [31]. The contact angle of the membrane surface decreased from 59.1° (for the PSF substrate) to 47.3° after TFC (thin film coating). The highest hydrophilic property, 20.7°, belongs to the membrane containing *H. elongata* aquaporin with His-tag (Supplementary file Table S1). In this study, we have used two *H. elongata* aquaporin expressed with different purification tags. GST tag is much longer than His-tag and it was observed that the presence of long-tail affected the surface characteristics of the aquaporin incorporated membrane by decreasing its hydrophilicity.

FTIR spectrum of membranes seen in Fig. 3 indicates the presence of proteoliposomes on membrane surface. The abundance of aquaporin in the membrane resulted in a significant increase in the volume of aromatic polyamides and displayed characteristic amide I, aromatic amide, and amide II bands at 1663 cm^{-1}, 1609 cm^{-1}, 1541 cm^{-1}, respectively. The 1701 cm^{-1} peak on the ordinate indicates the presence of phosphate I in the lipid bilayer of the aquaporin vesicles. Additionally, for the 2700–3300 cm^{-1} region, FTIR imaging of the membranes demonstrated the existence of lipid tails of liposomes at wavenumbers of 2959 and

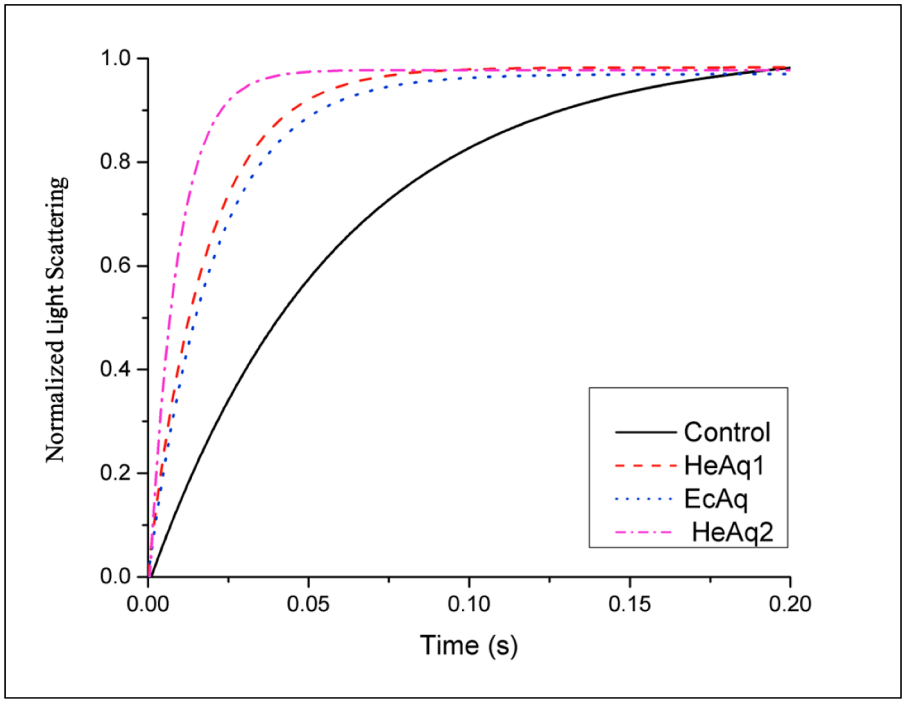

Fig. 2. Normalized light scattering of Control (empty), HeAq1, EcAq, and HeAq2 containing liposomes (Osmolite: 0.85 M NaCl; size: 200 nm DOPC).

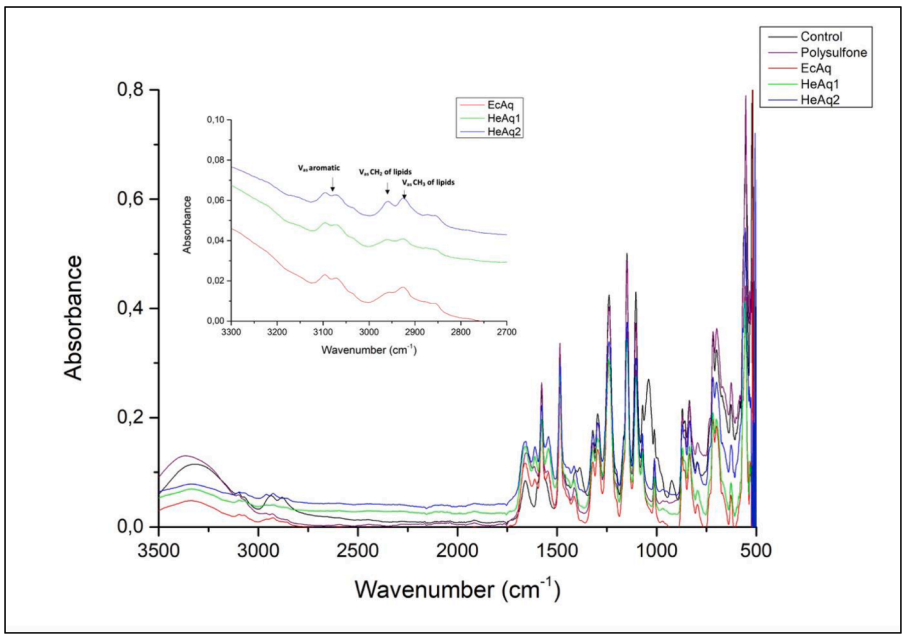

Fig. 3. ATR-FTIR spectra of membranes including PSF base layer membrane, control membrane with liposomes, and biomimetic membranes with proteoliposomes carrying aquaporins. Characteristics bonding patterns of lipids and amino acids are observed between 2900 and 3000 and 3050–3100 cm^{-1}.

2970 cm^{-1} [32].

Pore size analysis of the membranes was performed with Quantachrome Porometer 3 G ZH analysis. The mean pore size of the control membrane with empty liposomes (without aquaporin) and membrane with proteoliposomes (with aquaporin) were measured to be 183.2 nm and 123.6 nm, respectively (Figure S4). In studies performed with aquaporin-based membranes in the literature, the pore size of the membranes changes between 30 and 500 nm [33–35]. The pore sizes of TMC membranes prepared in this study are within this range.

The surface of the liposome-free membrane and proteoliposome-containing membranes were also visualized by SEM. Fig. 4. B shows the structure of the TMC-MPD layer which forms a thin film layer on the membrane surface. It was observed that liposomes are successfully incorporated into this thin film layer (Fig. 4C). A close view of liposomes could be observed in the micrograph showing cross-section of the membrane (Fig. 4D).

Surfaces of used and unused membranes can be seen in Fig. 4E and F, respectively. The fouling on the surface of membrane used for a year is noticeable. In spite of fouling water flux through this membrane has not decreased. On the other hand, its micropollutant rejection efficiency decreased dramatically (Table 6). The surface of the unused membrane in Fig. 4F, which was stored for one year period, is seen rather clean. No filtration was performed with this membrane.

3.3. Salt separation performance of membranes

The salt rejection potential of the membranes was first measured in order to determine their functionality. A dead-end filtration cell reactor was used to test the separation performance of biomimetic membranes using a 100 mM NaCl solution. Table S2 shows the results of filtration experiments performed with two sets of membranes, each membrane set has its own control membrane. In these salt filtration experiments, the J value (water flux) of *H. elongata* aquaporin-containing membranes were found to be higher than that of *E. coli* aquaporin incorporated membrane ($p < 0.05$). It was observed that His-tagged *H. elongata* aquaporin provides higher water flux (J) and salt rejection (%R) capacity to the thin film composite membrane ($p < 0.05$) as compared to GST-tagged one. The results of the present study supported previous findings [20].

3.4. Micropollutant rejection performance of membranes

Membranes were tested at RO mode for determination of their rejection performance for four different micropollutants (triclosan, terbutryn, diuron, and atrazine) mixed at two different concentrations (100 and 500 µg/L each). Membranes gained rejection capability after covering their surface with a thin film, even no aquaporins were incorporated in the structure. The polysulfone membranes coated with TMC layer including empty liposomes (control membranes) achieved 25–44% rejection depending on the micropollutant, and its water flow rate was lower than aquaporin-containing ones. The incorporation of aquaporins into the membrane surface increased the rejection capacity of the membranes. When atrazine, terbutryn, triclosan, and diuron at concentrations of 100 µg/L were filtered,% rejection of the aquaporin membranes varied between 66.7% and 90.3% depending on the type of aquaporin and micropollutant while the control membrane without aquaporin provides only 20.6–40.5% rejection. As micropollutant concentrations increased to 500 µg/L, membrane rejection rate decreased to 6% for aquaporin-free membranes and 36.4% for aquaporin-containing biomimetic membranes. For terbutryn and atrazine, membrane with *H. elongata* aquaporin showed higher rejection performance and improvement due to aquaporin incorporation is much more obvious when the concentration of chemicals increased to 0.5 mg/L (Fig. 5A). Halophilic aquaporin from *H. elongata* provided higher water flux ability to the membrane as compared to its mesophilic counterpart from *E. coli*. High treatment performances of 0.776 and 0.793 mg/m^2.h were observed for atrazine and terbutryn, respectively, with a membrane containing *H. elongata* aquaporin. Detailed data including water flux (*Jv*) and concentration of chemicals in the effluent can be found in the Supplementary file (Table S3-S4).

Three-dimensional structure and water channel pore (transmembrane pore) position of *E. coli* and *H. elongata* aquaporins were modeled with the Schrödinger Maestro program (Figure S1). The channel length-channel diameter of *E. coli* aquaporin and *H. elongata* aquaporin were calculated as 55.7 Å- 0.3 Å, 32.4 Å- 0.6 Å by the MoleOnline program, respectively (Table S5). Increase in water flux might be related to the shorter channel length and wider channel diameter of *H. elongata* aquaporin. Docking of micropollutants with aquaporins was performed by 3D modeling (Figure S2-S3, Table S5).

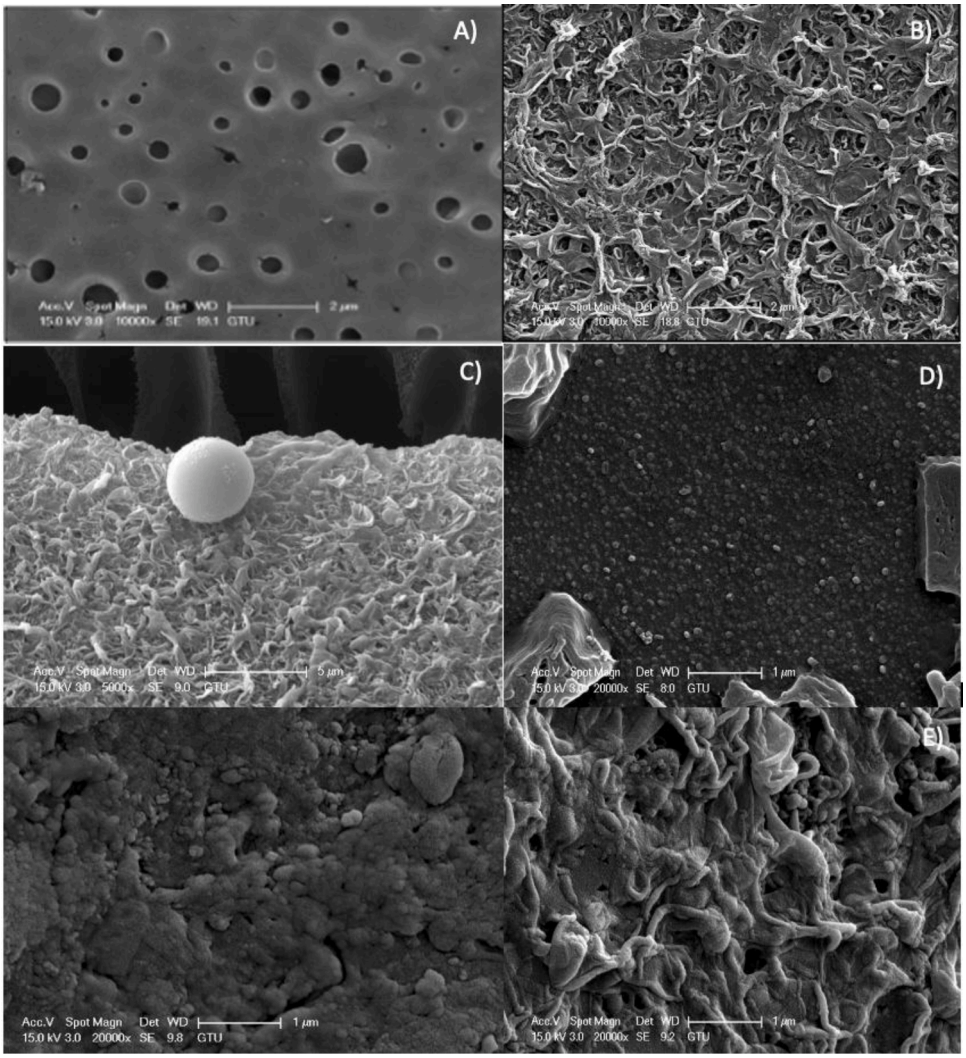

Fig. 4. SEM micrographs of the membranes. A) Surface of polysulfone base membrane B) Surface of polysulfone membrane coated with thin-film layer without liposomes, C) An intact liposome in thin-film layer (a cross-section cut), D) Surface of TFC membrane with embedded proteoliposomes, E) fouling on used membranes for a year period F) unused membranes stored for a year period.

Micropollutants can bind to the periphery or transmembrane pore channel amino acid residues. However binding positions of micropollutants on aquaporins seemed to have no effect on their rejection by the aquaporin incorporated membranes.

In Fig. 5B, the performance of membranes with halophilic *H. elongata* aquaporin with two different affinity tails are seen. The presence of a GST affinity tail in the aquaporin is shown to be an advantage for obtaining a high rejection value (%R)Eqn 5. However, membrane performance should be evaluated not only with its %R but also with flux (J) value. The effect of aquaporins on flux is an important phenomenon, resulting in the improvement of process efficiency with the treatment of a higher volume of influents. Flux improvement with the help of aquaporins has opened the difference between J_R values of control and aquaporin-containing membranes. Table 4 shows flux-dependent rejection (J_R) performances of the membranes.

Table 5 shows the physicochemical properties of the micropollutants and % rejection by the membrane with *H. elongata* aquaporin. Rejection rates for micropollutants with more methyl branching (atrazine and terbutryn) was found to be higher than others. The rejection rate was calculated to be lowest for diuron which has the highest pKa value among the filtered micropollutants. A number of chlorines in the structure seem to be not very effective on the rejection rate of the membranes.

3.5. Stability and shelf-life of membranes

The stability of the *E. coli* aquaporin-containing membrane and control membrane were compared in terms of their atrazine removal efficiency. In this experiment, the feed solution contained only 100 µg/L atrazine. Membranes are usually stabilized and reach their optimum performance several filtrations after their first usage.% rejection increased to 48.8% in third and fourth filtration by *E. coli* aquaporin incorporated membrane. As can be seen in Table 6, after 4 and 6 months period there is no remarkable decrease in the flux and in the rejection rate of the membrane for atrazine (44,6% rejection). However, after a year period (24 atrazine filtration in total)% rejection of aquaporin-containing membrane decreased to 10%.

4. Discussion

Industrialization has necessitated the production and use of an enormous amount of toxic chemicals. Micropollutants including active components of pesticides or medicines are widely used and detected in wastewater effluents. Das *et al.* (2017) compared concentrations of a large number of micropollutants in the effluent of different wastewater treatment facilities. Although they are expected to be present at trace quantities, it was reported that some of the micropollutants can be found

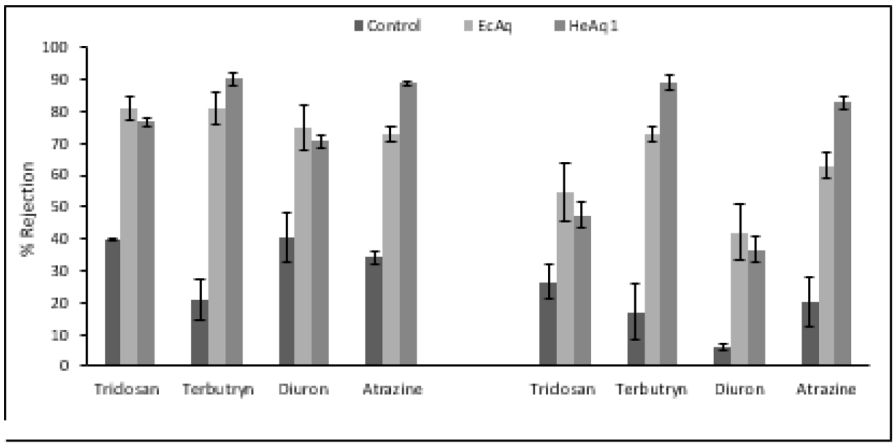

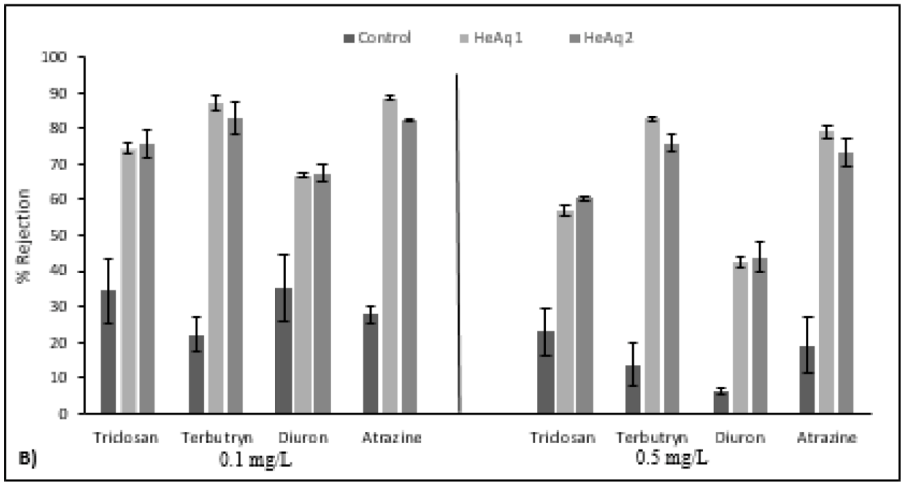

Fig. 5. Removal efficiencies of biomimetic thin-film layer composite membranes for different concentrations of micropolluants (0.1 mg/L and 0.5 mg/L). A) Removal efficiencies of membranes containing GST tagged .H. elonagate and E. coli equaporins. As micropolluants concentrations increased rejection rate of membranes decreased. The rejection rate for triclosan and diuron decreased when :he feed contains higher concentrations of micropolluants 0.5 mg/L). B) Removal efficiencies of memhranes containing His-tagged (HeAq2) and GST tagged (HeAq1: H. elongata aquaporins. Use of GET tag for aquaporin purification can be regarded as more effective as compared to His-tag for the activity of aquaporin on the membrane surface (high rejection rates for terbutryn and atrazine were obtained at two different concentrations of micropolluants).

Table 4
Flux-dependent rejection of the aquaporin incorporated TFC membranes.

	Flux dependent rejection (mg/m^{2}h) $J_R = (C_{inf} - C_{eff}) \times J_v$							
	0.1 mg/L feed concentration				0.5 mg/L feed concentration			
	Atrazine	Diuron	Tebutryn	Triclosan	Atrazine	Diuron	Tebutryn	Triclosan
Control	0.148	0.172	0.088	0.180	0.315	0.097	0.258	0.685
EcAq	0.488	0,496	0.543	0.576	2.103	1.401	2.370	2.400
HeAq1	0.776	0.613	0.793	0.708	3.195	1.403	3.333	2.500
Control	0.153	0.195	0.121	0.194	0.388	0.132	0.280	0.464
HeAq1	0.698	0.523	0.686	0.617	2.780	1.486	2.902	1.996
HeAq2	0.733	0.596	0.733	0.702	2.794	1.635	2.851	2.271

*GST tagged *E. coli* aquaporin (EcAq), *H. elongata* aquaporin (HeAq1), and His-tag carrying *H. elongata* aquaporin (HeAq2).

at very high concentrations in some effluents. For example, triclosan and diuron concentrations can be around 100 μg/L and diclofenac can be measured approximately 700 μg/L [43]. Degradation of micropollutants by microorganisms is hard due to their toxic nature and they cannot be eliminated efficiently during conventional wastewater treatment. Advanced treatment technologies are required, and novel processes are being developed for this aim. Processes like bioremediation by effective microorganisms, adsorption on activated carbon, oxidation processes [7, 8, 9], and membrane bioreactors have been used for the elimination of micropollutants from wastewater.

In the last 20 years, studies on the modification of membranes with biological molecules have increased and new usage areas have been discovered. Research on micropollutant removal with aquaporin-based membranes so far are listed in Table 7. Number of micropollutant removal studies with aquaporin based membranes have accelerated in the last decade, even pilot reactors were begun to be operated with aquaporin-based membranes [35]. Rapid water transfer ensures that aquaporin-based membranes may theoretically have very high permeability compared with conventional membranes. From the point of view of micropollutant removal, the combination of strong permeability and precise transport of water is rather important, as it provides quick absorption of even tiny trace organics without compromising flux [44]. Table 7 compares the mode of operation, method of fabrication, and also type of micropollutants filtered with thin film composite membranes and aquaporin based biomimetic membranes. Triclosan, a widely used antimicrobial agent, and herbicide atrazine are commonly chosen micropollutants in the studies performed with the aquaporin incorporated membranes. Different membrane technologies can be preferred in

Table 5
The physicochemical properties of the micropollutants and% rejection values of the membrane with *H.elongata* aquaporin.

Chemical name	Three dimensional structure	Chemical property			HeAq1 %Rejection Concentration (0.5 mg/L each)
		Molecular weight (g/mol)	pKa	LogD	
Atrazine	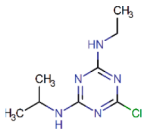	215.69	4.2	2.20	82.8
Diuron	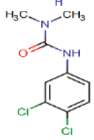	233.09	13.18	2.53	36.48
Terbutryn	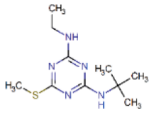	241.36	6.72	2.8	89.1
Triclosan	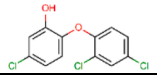	285.54	7.68	4.8	47.32

*Chemicalize program was used to determine the chemical properties. Chemicals with LogD values <3.0 at pH7.4 are hydrophilic and those with>3.0 at pH7.4 are hydrophobic. HeAq1: Membrane with GST tagged *H. elongata* aquaporin.

Table 6
Stability of the aquaporin incorporated TFC membrane.

Time	Control (membrane with no aquaporins)				Membrane with *E. coli* aquaporins			
	Jv (L/ m^2sa)	C_{eff} (mg/ L)	Flux dependent rejection (mg/ m^2.sa.)	% Rejection	Jv (L/ m^2sa)	C_{eff} (mg/ L)	Flux dependent rejection (mg/ m^2.sa.)	% Rejection
first day	7.9 ± 0.8	0.094	0.048	6.0	8.6 ± 0.9	0.075	0.218	25
4 months later	6.41 ± 0.9	0.082	0.115	18.0	9.1 ± 1.5	0.057	0.391	43.0
6 months later	9.95 ± 1,1	0.096	0.040	4.1	7.13 ± 0.09	0.055	0.43	44.6
12 months later *	6.22 ± 0.51	0.0991	0.007	1.0	7.21 ± 0.11	0.0845	0.11	15.5

* % rejection rate for 12-month-old membranes are mean of%R obtained in last three filtrations.

accordance with the process requirements. Membrane studies usually report the advantages of TFC membranes over CTA (cellulose triacetate) in terms of water flow, micropollutant rejection, and pH stability [34, 45]. In addition to membrane type, mode of operation is an important parameter affecting rejection rate. It is reported that FO membranes have some advantages over RO membranes. The use of osmotic gradient results in higher micropollutant rejection rates [46]. The use of pressure-operated nanofiltration (NF) membranes is favored for membrane processes, as they are effective in many conditions [47,48]. It is suggested that low-pressure reverse osmosis (LPRO) or RO membranes must be used instead of NF membranes to provide enough removal when the pollutants are small (200 g/mol). On the other hand, this high pressure used in the operation, which also raises the cost of removal due to the concentration polarization, results in the increased risk of contamination and blocking. Recently, the use of forward osmosis (FO) to solve these issues has gained interest [14,38]. Aquaporin-based membranes used in micropollutant removal studies were mostly operated in forward osmosis mode [33–35]. Xie and colleagues calculated how successful the flat sheet is at extracting various kinds of micropollutants with a wide range of hydrophilicity and charge [34]. 30 different micropollutants (2 μg/L each) including diclofenac, atrazine, and triclosan were mixed and filtered through a commercial aquaporin-based membrane operated on FO mode. Depending on the type of micropollutant, the rejection values of more than 90% was achieved**.** Engelhardt and his collaborators tested the first generation of hollow fiber aquaporin prototype and investigated the influence of micropollutants on the reversed permeability. A higher rejection of micropollutants and a higher water flux was achieved at the same time with aquaporin-based hollow fiber membrane [33]. The combination of different processes has potential to increase the efficiency of processes for micropollutant removal. Micropollutants including caffeine, paracetamol, salicylic acid, and other five micropollutants (0.5 ug/L each) was removed by PAC included MBR by Asif et al. (2020) [49]. It is reported that above%89 removals could be achieved.

It should be noted that all the micropollutant removal studies with aquaporin-based membranes in the literature were performed by using commercially available membranes containing *E. coli* aquaporin (Table 7). In the present study, the aquaporins were produced and purified and incorporated in thin film layer of the membranes in the laboratory. Membranes were tested in a dead-end reactor cell in a pressure-derived reverse osmosis mode. Rejection rate of membranes in our study is lower than that of commercially available membranes (Table 7). This might be caused by operation under pressure-driven RO mode. Imperfect laboratory conditions for membrane fabrication as compared to the automated systems of aquaporin-membrane producing companies might also affect the rejection rates. In our study, the performance of *H. elongata* aquaporin incorporated membrane was compared with that of *E. coli* aquaporin incorporated membrane. *H. elongata* aquaporin containing membrane rejected atrazine and terbutryn by 88.7 and 90.3% rejection rates, respectively. Membrane with *E. coli* aquaporin has a rejection rate of 80.8% for terbutryn. As compared to the *H. elongata* aquaporin-containing membranes, membrane with *E. coli* aquaporin has a slightly better rejection rate for diuron and triclosan, which are 74.9% and 80.1%, respectively (Table S3). Structure of halophilic aquaporin show differences in many parameters including channel pore diameter and length (Table S5). These characteristics of

Table 7
Application of aquaporin based membranes for micropollutant removal and comparison of their properties with other processes.

Other processes Process Type/Membrane Type	Source	Flux of DI water (L/m^2hbar)	Micropollutant Concentration (μg/L)	Flux of Mircpollutant mixture	Removal efficinency % R	Micropolutant Name*	Reference
Membrane studies							
FO membrane flat sheet (lab scale)	Hydration Technologies, Inc. (Albany, OR) and Dow FilmtecTM, Co. (Kentucky, USA)	0.54	500 in synthetic wastewater	–	60.2–90	Bisphenol A, **triclosan**, and diclofenac	[36]
(RO-TFC) Cellulose Triacetate Hollow fibre Bench-Scale	Toyobo Co., Ltd. (Osaka, Japan)	0.38	0.75 in synthetic wastewater	3.1	25–95%	41 TrOCs including **atrazine, diuron**	[37]
(FO-TFC) [38] (lab scale)	*E. coli* Aquaporin A/S (Lyngby, Denmark)	8.7	1000 in DI	–	97	**Atrazine,** 2,6-dichloro-benzamide (BAM) and desethyl-desisopropyl-atrazine (DEIA)	[38]
(FO-TFC) Hollowfiber membrane	*E. coli* Aquaporin A/S (Lyngby, Denmark)	7	1000 and 10,000 in DI	–	95–99	2,4-dichlorophenoxyacetic acid (2,4-D), bisphenol A (BPA), methylparaben	[33]
(FO-TFC) flat sheet	*E. coli* Aquaporin A/S (Lyngby, Denmark)	2.09	2		65–99	30 TrOCs including **atrazine, triclosan**.	[34]
(FO-TFC) flat-sheet (pilot scale) and hollow fiber membranes (lab scale)	*E. coli* Aquaporin A/S (Lyngby, Denmark)	1.5 for hollow fiber membrane 1.5 for flat sheet membrane	1000 in DI	15.1–13.9	93—98 for flat sheet 98 for hollow fiber	2–6 Dichloro-benzamide (BAM), 2-methyl-4-chlor-ophenoxyaceticacid (MCPA), and 2-(4-Chloro-2-(methylphenoxy) propionic acid (MCPP)	[35]
(FO-TFC) A flat-sheet membrane bioreactor	*E. coli* Aquaporin Asia, Singapore	1.5	5 synthetic wastewater	–	90–99	30 TrOCs including **atrazine, triclosan**.	[14]
(FO-TCF) hollow fiber membrane	*E. coli* Aquaporin A/S (Lyngby, Denmark)	1.2	1000 in DI	–	98.4–98.8	Naproxen and diclofenac	[39]
(FO-TCF) flat sheet membrane	*E. coli* Aquaporin A/S (Lyngby, Denmark)	1.2	10 in DI	–	96–99 lab-scale 80–99 pilot scale	35 TrOCs	[40]
(RO-TFC) flat sheet (lab scale)	*H. elongata* aquaporin Interfacial polymerization at a laboratory	1.75–1.28	500 and 100 in DI	8.86–7.89 for 0.1 mg/L (MP Conc.) 6.99–7.55 0.5 mg/L (MP Conc.)	66.7–90.3 (0.1 mg/L MP), 36.48–89.1 (0.5 mg/L MP)	Atrazine, diuron, terbutryn, triclosan	**ThisStudy**

Other processes Process	Reactor volume and process period	Micropollutant Concentration (μg/L)	Removal efficiency%R	Micropolutant Name	Reference
Biodegradation by *Phanerochaete chrysosporium*	Lab scale/12days	7	94% in 10 days	**Diuron**	[41]
Adsorption polyvinylpyrrolidone (PVP)-coated magnetite nanoparticle	50 mL sealed glass vial/30 min	25–250	>89% in 35 min	Tonalide, Bisphenol-A, **Triclosan**, Metolachlor, Ketoprofen, and Estriol	[42]

*Micropollutants written in bold are used in this study.

aquaporins revealed by 3D programs might be useful to understand variations in aquaporin performances. According to the Mole Online program, the channel length of *E. coli* aquaporin was longer and narrower as compared to *H. elongata* aquaporin. The higher rate of water flow of *H. elongata* aquaporin compared to *E. coli* aquaporin can be associated with the width of the transmembrane channel pore (Figure S1). Interaction of micropollutants with aquaporins may also affect their rejection by aquaporin-containing filtration membranes. The binding properties of micropollutants to the aquaporins were investigated by Schrodinger Maestro protein modeling program (Table S6). 3D modeling revealed that the micropollutants terbutryn and triclosan bind to the amino acids that are located in the *E. coli* aquaporin transmembrane channel pore. Nonetheless, it is hard to find a direct relation between micropollutants rejection performance and aquaporin structure or micropollutant structure. The rejection of micropollutants seems to be affected by many parameters including pore size and hydrophilicity of membranes. Halophilic aquaporin incorporated membranes showed slightly better performance at especially high

concentrations of micropollutants. Hydrophilicity (logD value), acidic or basic characteristics (pKa values), and three-dimensional structure of the micropollutants might also have effect on rejection (Table 5).

Coday et al. [50] reported that different factors including size, steric effect, charge of micropollutant, and also a type of membrane and operation mode play a role on micropollutant rejection performances of the membranes. It is reported that in RO mode, electrostatic interactions play a dominant role in governing the rejection of charged micropollutants. In FO and PRO (pressure retarded osmosis) modes, the rejection of charged micropollutants was governed by both electrostatic interaction and size exclusion, while rejection of neutral compounds was dominated by size exclusion [51]. In the present study, *H. elongata* aquaporin incorporated membranes were found to be more efficient in rejecting terbutryn and atrazine. These substances have CH_3 branching in their structure. Branching in the chemical structure which results in steric effect seems to be an important parameter. On the other hand, the rejection of diuron with a relatively high pKa value was found to be lower (Table 5). The effect of ionization potential of the chemical on removal efficiency should not be underestimated. Membrane pore size analysis showed that pore size of liposome incorporated membrane was reduced when aquaporins were incorporated into the membrane structure. Aquaporin incorporated membrane water flux is always found to be higher than the control membranes (Table S2), which means that water flux through membranes is not related only to pore size but also related with the nature of aquaporin. However, rejection for all of the tested micropollutants is increased with aquaporin incorporation into the membrane structure. This result can be attributed to smaller pore size obtained after the addition of aquaporins into the membrane surface. Smaller pore size seems to be a primarily important parameter affecting the micropollutant rejection rate.

As previous studies in the literature and also the present study show, aquaporin incorporation into membrane structure increases water permeability of the membranes. However, it was realized that perfect water permeation capacity of aquaporins can not be maximally utilized in aquaporin-based membranes. The decrease in the performance of aquaporins upon incorporation on membrane surface was calculated for GST-tagged *H. elongata* aquaporin used in this study. For the determination of water permeability for a single aquaporin on membrane surface operated in a dead-end filtration cell, water permeability increase due to the presence of aquaporin (GST-HeAqp) on membrane was calculated. When we assume that all the aquaporins used for proteoliposome preparation were successfully inserted into the the membrane surface, water permeability per single aquaporin on membrane surface was determined to be 7.15×10^{-17} cm^3/s (calculation can be found in the Supplementary file related to Table S2). P_f value for GST-HeAq, which is calculated from stop flow measurements (8.21×10^{-14} cm^3/s), is much more higher than 7.15×10^{-17} cm^3/s. As compared to the theoretical estimation based on stop flow P_f values, there was a hundredfold decrease in the performance of aquaporins when incorporated on membrane surface. This decrease in aquaporin performance can be attributed to many factors. Firstly, difference in operation mechanisms of the stopped-flow light scattering measurements and dead-end filtration systems has to be considered. The other effects may be related to membrane preparation methods. Embedding aquaporins into thin film layers might affect aquaporins activity due to the presence of different chemical substances used to prepare thin layer. Besides, some of the aquaporins might not allow water passage since they remain beneath the thin film layer. It may be possible to increase aquaporin performance on membrane surfaces by optimization of membrane fabrication methods. The use of different embedding chemicals other than TMC for thin layer preparation, use of different functionalizing agents instead of MPD, such as graphene oxide may change aquaporin functionality. Moreover, based membrane materials and coating methods can also affect aquaporin concentration that can be inserted on membrane surface. For example, a spin coating can be applied for more efficient thin layer preparation instead of immersing membranes into the proteoliposome solution. Optimization of TMC-MPD concentrations can also be considered to increase aquaporin performance on biomimetic membranes.

The stability and shelf life of the aquaporin incorporated membrane was analyzed using *E. coli* aquaporin incorporated membrane as the test membrane and atrazine as the test chemical. It was observed that the membrane lost its micropollutant repelling property in a year period,% rejection for atrazine dropped to 10% at 24^{th} filtration after one year. Results for 4 and 6-month-old membrane was satisfying that there was no remarkable decrease in % rejection rate for atrazine in this period. It was also noticed that when atrazine is a sole chemical in the solution, the % rejection rate of the membranes for this compound was lower as compared to filtration of a mixture of compounds. The water flux value of one year old membranes did not show a dramatic increase which suggests that there is no disruption in the membrane structure including thin film layer or polysulfone base. The SEM micrographs show that there is a thick cake layer on 12-month-old membrane used 24 times for atrazine filtration. Chemical artifacts accumulated on the surface might have affected chemical interaction between membrane surface and the micropollutant, resulting in the disability of the membrane in micropollutant rejection. This result also shows that repelling of micropollutants by membranes is not only dependent on size exclusion. Electrostatic interactions which can be affected by properties of the TMC-MPD chemical layer, liposome, and aquaporin proteins may play important role in the filtration of micropollutants.

In this research, the effect of affinity tails linked to the aquaporin protein on the micropollutant rejection capacity of the membranes was also analyzed. Affinity tails are linked to the genes coding for proteins during cloning and they are purified in accordance with the requirements of these affinity tails. Length of affinity tails used in this study is 6 histidine amino acid residues for His-tag and 211amino acid residue for GST tag. There is no remarkable difference in the rejection rates due to the different affinity tails. A slight increase was observed for terbutryn and atrazine with GST tagged *H. elongata* aquaporin. GST tagged and His-tagged *H. elongata* aquaporins resulted in %87.2 and % 82.7 rejection rates for 100 μg/L terbutryn when incorporated in membranes (Fig. 5). Nonetheless, water flux is affected by type of tags linked to the aquaporins, which affects flux dependent rejection rate of the process (Table S4).

Aquaporin incorporation into the membrane structure both results in increase in water flux of thin film composite membranes and provides reasonable rejection performance. Various factors including pore size, hydrophilicity, and mode of operation play important roles in rejection performances of the membranes. Although not as much as the membrane structure, micropollutant chemical characteristics such as charge or hydrophilicity is also effective on rejection rates.

There are many applications of aquaporin-based membrane technologies in a variety of sectors for separation processes including treatment of sugarcane molasses distillery wastewater, coconut milk concentration, algae dewatering in algal harvesting with low energy requirement, and multifiltration bed system in the International Space Station (ISS) Water Processor Assembly (WPA)[52]. They are needed especially for the recovery of value-added products. Therefore, studies on biomimetic and bio-inspired membranes are increasing day by day. Apart from biological membrane proteins such as aquaporin, artificial water channels, carbon nanotubes and metal-organic frameworks (MOFs) have begun to be used in the fabrication of membranes [53]. These functional components are used to imitate biological water channels, increase the water flow rate, and provide the durability of the channels on the membrane. Studies performed so far have shown that aquaporin-based biomimetic membranes have a high potential for salt removal from aqueous environments. Recent research on micropollutant removal with these membranes have presented their capacity for the treatment of toxic pollutants. In this study, type of aquaporins and affinity tags linked to them were shown to be effective on micropollutant rejection capacity of biomimetic membranes.

Declaration of Competing Interest

The authors declare that they have no known competing financial interests or personal relationships that could have appeared to influence the work reported in this paper.

Acknowledgments

We thank the Scientific and Technological Research Council of Turkey and YÖK for supporting this study (Project no: TÜBİTAK 119Y307, 115Z245, and YÖK 100/2000 doctoral scholarship program).

Supplementary materials

Supplementary material associated with this article can be found, in the online version, at doi:10.1016/j.btre.2022.e00745.

References

[1] F. Metz, K. Ingold, Sustainable wastewater management: is it possible to regulate micropollution in the future by learning from the past? A Policy Anal. Sustain. 6 (2014) https://doi.org/10.3390/su6041992.
[2] L. Goswami, R. Vinoth Kumar, S.N. Borah, N. Arul Manikandan, K. Pakshirajan, G. Pugazhenthi, Membrane bioreactor and integrated membrane bioreactor systems for micropollutant removal from wastewater: a review, J. Water Process Eng. (2018), https://doi.org/10.1016/j.jwpe.2018.10.024 https://doi.org/.
[3] K. Fent, A.A. Weston, D. Caminada, Ecotoxicology of human pharmaceuticals, Aquat. Toxicol. 76 (2006) 122–159.
[4] A. Pruden, R. Pei, H. Storteboom, K.H. Carlson, Antibiotic resistance genes as emerging contaminants: studies in northern Colorado, Environ. Sci. Technol. 40 (2006) 7445–7450.
[5] N. Bolong, A.F. Ismail, M.R. Salim, T. Matsuura, A review of the effects of emerging contaminants in wastewater and options for their removal, Desalination 239 (2009) 229–246.
[6] R. Guillossou, J.Le Roux, R. Mailler, C.S. Pereira-Derome, G. Varrault, A. Bressy, E. Vulliet, C. Morlay, F. Nauleau, V. Rocher, J. Gasperi, Influence of dissolved organic matter on the removal of 12 organic micropollutants from wastewater effluent by powdered activated carbon adsorption, Water Res. 172 (2020), 115487, https://doi.org/10.1016/J.WATRES.2020.115487 https://doi.org/.
[7] A.I. Schäfer, I. Akanyeti, A.J.C. Semião, Micropollutant sorption to membrane polymers: a review of mechanisms for estrogens, Adv. Colloid Interface Sci. 164 (2011) 100–117, https://doi.org/10.1016/j.cis.2010.09.006, https://doi.org/.
[8] A. Ratnasari, A. Syafiuddin, N.S. Zaidi, A.B. Hong Kueh, T. Hadibarata, D. D. Prastyo, R. Ravikumar, P. Sathishkumar, Bioremediation of micropollutants using living and non-living algae - Current perspectives and challenges, Environ. Pollut. (2022) 292, https://doi.org/10.1016/J.ENVPOL.2021.118474.
[9] H.T. Nguyen, Y. Yoon, H.H. Ngo, A. Jang, The application of microalgae in removing organic micropollutants in wastewater, 51 (2020) 1187–1220. 10.1080/10643389.2020.1753633.
[10] W. Ma, Y. Li, M. Zhang, S. Gao, J. Cui, C. Huang, G. Fu, Biomimetic durable multifunctional self-cleaning nanofibrous membrane with outstanding oil/water separation, photodegradation of organic contaminants, and antibacterial performances, ACS Appl. Mater. Interfaces. 12 (2020) 34999–35010, https://doi.org/10.1021/ACSAMI.0C09059/SUPPL_FILE/AM0C09059_SI_001.PDF, https://doi.org/.
[11] V. Sharma, G. Borkute, S.P. Gumfekar, Biomimetic nanofiltration membranes: critical review of materials, structures, and applications to water purification, Chem. Eng. J. 433 (2022), 133823, https://doi.org/10.1016/J.CEJ.2021.133823 https://doi.org/.
[12] Y. xiao Shen, P.O. Saboe, I.T. Sines, M. Erbakan, M. Kumar, Biomimetic membranes: a review, J. Memb. Sci. 454 (2014) 359–381, https://doi.org/10.1016/J.MEMSCI.2013.12.019, https://doi.org/.
[13] G. Benga, On the definition, nomenclature and classification of water channel proteins (aquaporins and relatives), Mol. Aspects Med. 33 (2012) 514–517.
[14] W. Luo, M. Xie, X. Song, W. Guo, H.H. Ngo, J.L. Zhou, L.D. Nghiem, Biomimetic aquaporin membranes for osmotic membrane bioreactors: membrane performance and contaminant removal, Bioresour. Technol. 249 (2018) 62–68.
[15] X. Li, S. Chou, R. Wang, L. Shi, W. Fang, G. Chaitra, C.Y. Tang, J. Torres, X. Hu, A. G. Fane, Nature gives the best solution for desalination: aquaporin-based hollow fiber composite membrane with superior performance, J. Memb. Sci. 494 (2015) 68–77.
[16] L. Xia, M.F. Andersen, C. Hélix-Nielsen, J.R. McCutcheon, Novel commercial aquaporin flat-sheet membrane for forward osmosis, Ind. Eng. Chem. Res. 56 (2017) 11919–11925, https://doi.org/10.1021/ACS.IECR.7B02368, https://doi.org/.
[17] P.S. Zhong, T.S. Chung, K. Jeyaseelan, A. Armugam, Aquaporin-embedded biomimetic membranes for nanofiltration, J. Memb. Sci. 407–408 (2012) 27–33, https://doi.org/10.1016/J.MEMSCI.2012.03.033, https://doi.org/.
[18] Y. Zhao, C. Qiu, X. Li, A. Vararattanavech, W. Shen, J. Torres, C. Hélix-Nielsen, R. Wang, X. Hu, A.G. Fane, C.Y. Tang, Synthesis of robust and high-performance aquaporin-based biomimetic membranes by interfacial polymerization-membrane preparation and RO performance characterization, J. Memb. Sci. 423–424 (2012) 422–428, https://doi.org/10.1016/J.MEMSCI.2012.08.039, https://doi.org/.
[19] Y. Chun, L. Qing, G. Sun, M.R. Bilad, A.G. Fane, T.H. Chong, Prototype aquaporin-based forward osmosis membrane: filtration properties and fouling resistance, Desalination 445 (2018) 75–84, https://doi.org/10.1016/J.DESAL.2018.07.030, https://doi.org/.
[20] N.G. Çalıcıoğlu, G.Ö. Özdemir, A. Öztürk, A. Yıldız, H. Yılmaz, P. Ergenekon, M. Erbakan, E. Erhan, M. Özkan, Use of halophilic aquaporin for preparation of biomimetic thin film composite membrane, J. Memb. Sci. 568 (2018) 105–112, https://doi.org/10.1016/j.memsci.2018.09.065, https://doi.org/.
[21] H. Yılmaz, F.İ. Özdemir, P. Ergenekon, M. Özkan, Affinity tag effect on the salt rejection potential of Halomonas elongata aquaporin incorporated in thin film nanocomposite membrane, Protein Expr. Purif. (2020) 173, https://doi.org/10.1016/j.pep.2020.105664, https://doi.org/.
[22] M.M. Bradford, A rapid and sensitive method for the quantitation of microgram quantities of protein utilizing the principle of protein-dye binding, Anal. Biochem. 72 (1976) 248–254. https://www.sciencedirect.com/science/article/pii/0003269776905273 (accessed January 31, 2021).
[23] M.C. Woodle, D. Papahadjopoulos, Liposome preparation and size characterization, Methods Enzymol. 171 (1989) 193–217, https://doi.org/10.1016/S0076-6879(89)71012-0, https://doi.org/.
[24] C. Hannesschläger, T. Barta, C. Siligan, A. Horner, Quantification of water flux in vesicular systems, (2018). https://doi.org/ 10.1038/s41598-018-26946-9.
[25] R. Sengur, C.F. de Lannoy, T. Turken, M. Wiesner, I. Koyuncu, Fabrication and characterization of hydroxylated and carboxylated multiwalled carbon nanotube/polyethersulfone (PES) nanocomposite hollow fiber membranes, Desalination 359 (2015) 123–140, https://doi.org/10.1016/J.DESAL.2014.12.040, https://doi.org/.
[26] K. Berka, O. Hanák, D. Sehnal, P. Banáš, V. Navrátilová, D. Jaiswal, C.M. Ionescu, R. Svobodová Vařeková, J. Koča, M. Otyepka, MOLEonline 2.0: interactive web-based analysis of biomacromolecular channels, Nucleic Acids Res. 40 (2012) W222–W227, https://doi.org/10.1093/NAR/GKS363, https://doi.org/.
[27] M. Erbakan, Y.X. Shen, M. Grzelakowski, P.J. Butler, M. Kumar, W.R. Curtis, Molecular cloning, overexpression and characterization of a novel water channel protein from rhodobacter sphaeroides, PLoS ONE 9 (2014) e86830, https://doi.org/10.1371/JOURNAL.PONE.0086830, https://doi.org/.
[28] H. Hadidi, R. Kamali, A. Binesh, Investigation of the aquaporin-2 gating mechanism with molecular dynamics simulations, Proteins Struct. Funct. Bioinforma. 89 (2021) 819–831, https://doi.org/10.1002/PROT.26061, https://doi.org/.
[29] M. Kumar, M. Grzelakowski, J. Zilles, M. Clark, W. Meier, Highly permeable polymeric membranes based on the incorporation of the functional water channel protein Aquaporin Z, Proc. Natl. Acad. Sci. 104 (2007) 20719–20724, https://doi.org/10.1073/PNAS.0708762104, https://doi.org/.
[30] M. Ben Amira, M. Faize, M. Karlsson, M. Dubey, M. Frąc, J. Panek, B. Fumanal, A. Gousset-Dupont, J.L. Julien, H. Chaar, D. Auguin, R. Mom, P. Label, J.S. Venisse, Fungal X-intrinsic protein aquaporin from trichoderma atroviride: structural and functional considerations, Biomol 11 (2021) 338, https://doi.org/10.3390/BIOM11020338. Page11 (2021) 338https://doi.org/.
[31] W. Ding, J. Cai, Z. Yu, Q. Wang, Z. Xu, Z. Wang, C. Gao, Fabrication of an aquaporin-based forward osmosis membrane through covalent bonding of a lipid bilayer to a microporous support, J. Mater. Chem. A. 3 (2015) 20118–20126, https://doi.org/10.1039/c5ta05751e, https://doi.org/.
[32] Z. Movasaghi, S. Rehman, I.U. Rehman, Fourier transform infrared (FTIR) spectroscopy of biological tissues, Appl. Spectrosc. Rev. 43 (2008) 134–179, https://doi.org/10.1080/05704920701829043, https://doi.org/.
[33] S. Engelhardt, A. Sadek, S. Duirk, Rejection of trace organic water contaminants by an Aquaporin-based biomimetic hollow fiber membrane, Sep. Purif. Technol. (2018), https://doi.org/10.1016/j.seppur.2017.12.061 https://doi.org/.
[34] M. Xie, W. Luo, H. Guo, L.D. Nghiem, C.Y. Tang, S.R. Gray, Trace organic contaminant rejection by aquaporin forward osmosis membrane: transport mechanisms and membrane stability, Water Res. (2018), https://doi.org/10.1016/j.watres.2017.12.072 https://doi.org/.
[35] M. Nikbakht Fini, H.T. Madsen, J.L. Sørensen, J. Muff, Moving from lab to pilot scale in forward osmosis for pesticides rejection using aquaporin membranes, Sep. Purif. Technol. (2020) 240, https://doi.org/10.1016/j.seppur.2020.116616, https://doi.org/.
[36] M. Xie, L.D. Nghiem, W.E. Price, M. Elimelech, Comparison of the removal of hydrophobic trace organic contaminants by forward osmosis and reverse osmosis, Water Res. 46 (2012) 2683–2692, https://doi.org/10.1016/J.WATRES.2012.02.023, https://doi.org/.
[37] T. Fujioka, S.J. Khan, J.A. McDonald, L.D. Nghiem, Rejection of trace organic chemicals by a hollow fibre cellulose triacetate reverse osmosis membrane, Desalination 368 (2015) 69–75, https://doi.org/10.1016/J.DESAL.2014.06.011, https://doi.org/.
[38] H.T. MAdsen, N. Bajraktari, C. Hélix-Nielsen, B. Van der Bruggen, E.G. Søgaard, Use of biomimetic forward osmosis membrane for trace organics removal, J. Memb. Sci. (2015), https://doi.org/10.1016/j.memsci.2014.11.055 https://doi.org/.
[39] I. Petrinic, H. Bukšek, I. Galambos, R. Gerencsér-Berta, M.S. Sheldon, C. Helix-Nielsen, Removal of naproxen and diclofenac using an aquaporin hollow fibre forward osmosis module, Deswater.Com. 192 (2020) 415–423, https://doi.org/10.5004/dwt.2020.26082, https://doi.org/.
[40] R. Li, S. Braekevelt, J.L.N. De Carfort, S. Hussain, U.E. Bollmann, K. Bester, Laboratory and pilot evaluation of aquaporin-based forward osmosis membranes

for rejection of micropollutants, Water Res. 194 (2021), 116924, https://doi.org/10.1016/J.WATRES.2021.116924 https://doi.org/.
[41] J.D.S. Coelho-Moreira, A. Bracht, A.C. Da Silva De Souza, R.F. Oliveira, A.B. De Sá-Nakanishi, C.G.M. De Souza, R.M. Peralta, Degradation of diuron by phanerochaete chrysosporium: role of ligninolytic enzymes and cytochrome P450, Biomed Res. Int. 2013 (2013), https://doi.org/10.1155/2013/251354 https://doi.org/.
[42] M. Alizadeh Fard, A. Vosoogh, B. Barkdoll, B. Aminzadeh, Using polymer coated nanoparticles for adsorption of micropollutants from water, Colloids Surfaces A Physicochem. Eng. Asp. 531 (2017) 189–197, https://doi.org/10.1016/J.COLSURFA.2017.08.008, https://doi.org/.
[43] S. Das, N.M. Ray, J. Wan, A. Khan, T. Chakraborty, M.B. Ray, Micropollutants in wastewater: fate and removal processes. Physico-Chemical Wastewater Treat, Resour. Recover., InTech, 2017, https://doi.org/10.5772/65644 https://doi.org/.
[44] C.Y. Tang, Y. Zhao, R. Wang, C. Hélix-Nielsen, A.G. Fane, Desalination by biomimetic aquaporin membranes: review of status and prospects, Desalination (2013), https://doi.org/10.1016/j.desal.2012.07.007 https://doi.org/.
[45] X. Jin, J. Shan, C. Wang, J. Wei, C.Y. Tang, Rejection of pharmaceuticals by forward osmosis membranes, J. Hazard. Mater. 227 (2012) 55–61.
[46] A. D'Haese, P. Le-Clech, S. Van Nevel, K. Verbeken, E.R. Cornelissen, S.J. Khan, A. R.D. Verliefde, Trace organic solutes in closed-loop forward osmosis applications: influence of membrane fouling and modeling of solute build-up, Water Res (2013), https://doi.org/10.1016/j.watres.2013.06.006 https://doi.org/.
[47] A. Karabelas, K. Plakas, Membrane treatment of potable water for pesticides removal. Herbic. Theory Appl., InTech, 2011.
[48] K.V. Plakas, A.J. Karabelas, Removal of pesticides from water by NF and RO membranes—A review, Desalination 287 (2012) 255–265.
[49] M.B. Asif, B. Ren, C. Li, T. Maqbool, X. Zhang, Z. Zhang, Powdered activated carbon – Membrane bioreactor (PAC-MBR): impacts of high PAC concentration on micropollutant removal and microbial communities, Sci. Total Environ. 745 (2020), 141090, https://doi.org/10.1016/J.SCITOTENV.2020.141090 https://doi.org/.
[50] B.D. Coday, B.G.M. Yaffe, P. Xu, T.Y. Cath, Rejection of trace organic compounds by forward osmosis membranes: a literature review, Environ. Sci. Technol. (2014), https://doi.org/10.1021/es4038676 https://doi.org/.
[51] A.A. Alturki, J.A. McDonald, S.J. Khan, W.E. Price, L.D. Nghiem, M. Elimelech, Removal of trace organic contaminants by the forward osmosis process, Sep. Purif. Technol. 103 (2013) 258–266.
[52] P. Wagh, I.C. Escobar, Biomimetic and bioinspired membranes for water purification: a critical review and future directions, Environ. Prog. Sustain. Energy. 38 (2019) e13215, https://doi.org/10.1002/EP.13215, https://doi.org/.
[53] Y.M. Tu, L. Samineni, T. Ren, A.B. Schantz, W. Song, S. Sharma, M. Kumar, Prospective applications of nanometer-scale pore size biomimetic and bioinspired membranes, J. Memb. Sci. 620 (2021), 118968, https://doi.org/10.1016/J.MEMSCI.2020.118968 https://doi.org/.